



Journal of Applied and Computational Mechanics



Research Paper

Modeling beam-like planar structures by a one-dimensional continuum: an analytical-numerical method

Manuel Ferretti^{1,2}, Francesco D'Annibale^{1,2}, Angelo Luongo^{1,2}*

¹Department of Civil, Construction-Architectural and Environmental Engineering, University of L'Aquila, 67100 L'Aquila, Italy, Email: manuel.ferretti@univaq.it

²International Research Center on Mathematics and Mechanics of Complex Systems, University of L'Aquila, 67100, L'Aquila, Italy, Email: francesco.dannibale@univaq.it

Received March 31 2020; Revised May 07 2020; Accepted for publication May 07 2020.

Corresponding author: Angelo Luongo (angelo.luongo@univaq.it)

© 2021 Published by Shahid Chamran University of Ahvaz

Abstract. In this paper, beam-like structures, macroscopically behaving as planar Timoshenko beams, are considered. Planar frames, made by periodic assemblies of micro-beams and columns, are taken as examples of these structures and the effectiveness of the equivalent beam model in describing their mechanical behavior, is investigated. The Timoshenko beam (coarse model) is formulated via the direct one-dimensional approach, by considering rigid cross-sections and flexible axis-line, while its constitutive laws is determined through a homogenization procedure. An identification algorithm for evaluation of the constitutive constants is illustrated, based on Finite Element analyses of the cell of the periodic system. The inertial properties of the equivalent model are instead analytically identified under the hypothesis the masses are lumped at the joints. The advantages in using the equivalent model are discussed with reference to the linear static and dynamic responses of some planar frames, taken as case-studies, for which both analytical and numerical tools are used. Numerical results, obtained by the equivalent model, are compared with Finite Element analyses on planar frames (fine models), considering both symmetric and not-symmetric layouts, in order to show to effectiveness of the proposed algorithm. A comparison with analytical results is carried out to validate the limits of applicability of the method.

Keywords: Beam-like structures, Equivalent beam model, Timoshenko beam, Homogenization procedure.

1. Introduction

Homogenization techniques are efficient tools to analyze periodic structures and micro-structured meta-materials (see, e.g., [1, 2, 3, 4, 5, 6, 7, 8, 9, 10]). Among these systems, tower buildings and multi-story frames can be modeled as generalized beam, if the interest is focused on their *overall mechanical behavior* [11, 12, 13, 14, 15, 16, 17, 18, 19, 20, 21, 22, 23, 24, 25, 26]. The main advantage to deal with one-dimensional equivalent models consists in the dramatic lowering of the number of degrees of freedom with respect to Finite Element method. Consequently, a lower computational effort is required in solving the elastic problem (see, e.g., [27, 28, 29]), or, more remarkably, closed-form solutions can be obtained in many applications.

Different up-scaling approaches can be pursued to determine the properties of the equivalent beam model. They can be roughly classified into: (i) *heuristic approaches* (see, e.g., [30, 31, 32]) in which the equivalent beam model is a-priori assumed, by renouncing to link the micro and macro quantities; (ii) *asymptotic homogenization approaches* (see, e.g., [3, 33]), in which the equivalent model (not necessarily representing a known continuum) is rigorously derived, together with the micro-macro relationships. However, there is a third approach, which has been proposed by the authors, namely, (iii) the *mixed-approach*, in which the continuum model is heuristically predicted, but the micro-macro relationships are analytically determined on the ground of energy balances.

The mixed approach has been successfully applied by the authors in dealing with periodic buildings and towers in the 3D-space, which have been macroscopically modeled either: (i) as shear-shear-torsional beams, or (ii) Timoshenko beams [18, 19, 20, 23, 34, 24, 25, 35]. Accordingly, the floors and columns of the periodic structures were respectively identified with the cross-sections and longitudinal fibers of the underlying continuous beam. Then, by enforcing strain energy equivalence between a cell of the periodic system and a segment of the continuous beam, analytical expressions were derived, linking the elastic constants at the micro- and macro-scales. Several mechanical problems were solved, both in the linear and nonlinear regime, namely: statics [20, 23], dynamics [20, 25], buckling [34, 35] and aeroelasticity, [18, 19, 24].

The mixed approach, however, suffers the need of introducing some strong assumptions about the stiffnesses of the floors, both in-plane and out-of plane, and of the columns, both axial and flexural. As a matter of fact, the Timoshenko beam requires the floors do not undergo membrane strains, nor warp out-of plane, thus limiting the applicability of the model. For these reasons, the (stronger) flexural rigidity assumption was critically reconsidered by the authors in [26], discussing planar frames. It was shown there, that, by resorting to the concepts of 'shear factor' and 'flexural factor' (as done to include the de Saint-Venant results in the Timoshenko beam theory), it is possible to account for the out-of plane true flexibility of the cross-section, even when a rigid cross-section model is heuristically adopted. Indeed, these *corrective factors*, suitably reduce the shear and flexural stiffnesses of the macro-model, by accounting on average (i.e. on an energy balance ground), for the neglected warping. Unfortunately, as highlighted in [26], also this approach is limited by the fact that simple analytical expressions for the corrective factors are obtainable only for geometrically regular frames, i.e. a rare occurrence in real applications.



In this paper, the analysis developed in [26] is complemented, by following an approach similar to that presented in [30]. Planar frames with general layout are considered as examples of beam-like structures, for which a Timoshenko beam model (coarse equivalent model) is adopted to describe their global mechanical behavior. The limit of applicability of the approach presented in [26] is overcome by implementing an energy-based numerical algorithm, aimed at evaluating the macroscopic elastic and inertial properties of the beam via a Finite Element (FE) analysis of a single cell of the frame. In this way, the floor warping is accounted in integral form, although the simplicity of the analytical micro-macro relationship is lost. Numerical examples, relevant to both linear statics and linear dynamics are developed. Both analytical and numerical tools are used, namely: (i) analytical solutions for the static problem, and, (ii) Finite Difference numerical solutions for dynamic analysis.

The paper is organized as follows. In Section 2. the fundamental equations of the macroscopic model are recalled. In Section 3. the identification procedures for elastic and inertial constants of this model are described; the analytical results of [26] are resumed. In Section 4. the analytical and numerical approaches are discussed for static and dynamic problems, respectively. In Section 5., comparisons between results provided by Finite Element models (fine models) and coarse model are developed. In Section 6. some conclusions are drawn. Finally an Appendix, containing the analytical expressions of the elastic constants, closes the paper.

2. The fully-coupled Timoshenko beam model

A planar multi-story frame, of width b and height ℓ , is considered as an example of a cellular beam-like structure (Fig. 1-a). It is composed of n flexible floors, connected by m flexible columns of the same height h , and possibly braced by hinged diagonal trusses, repeating themselves at each floor. A cell is made by: (i) two adjacent floors (each having half of the true stiffness), (ii) an order of columns segmenting the beams into $m - 1$ spans of length b_i , and (iii) trussed braces.

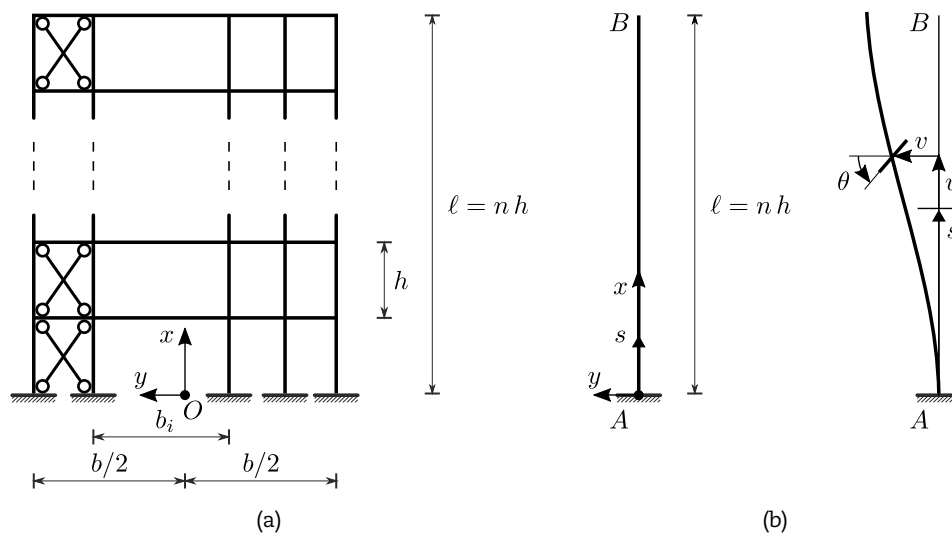


Fig. 1. Study object: (a) planar frame; (b) equivalent beam model.

A target one-dimensional continuum model is heuristically adopted, guided by the idea that the flexible floors and columns roughly behave as the cross-sections and the longitudinal fibers of a macroscopic beam, respectively. The 2D linear Timoshenko beam [36, 37, 38, 39, 40, 41] is chosen, in which the cross-section are assumed rigid and the axis-line flexible (Fig. 1-b). It is worth noticing that the rotation of the rigid cross-section of the Timoshenko beam must be meant as an averaged rotation of the warped cross-section of the real beam.

The choice of the model determines kinematics and equilibrium, while leaves free the constitutive law. Accordingly, the strain-displacement relationships read:

$$\varepsilon = u', \quad \gamma = v' - \theta, \quad \kappa = \theta', \quad (1)$$

linking the longitudinal displacement $u(s, t)$, the transverse displacement $v(s, t)$ and the rotation $\theta(s, t)$ to the elongation $\varepsilon(s, t)$, the shear strain $\gamma(s, t)$ and the curvature $\kappa(s, t)$; here $s \in [0, \ell]$ is the material abscissa, t the time, and a prime denotes space-differentiation. Moreover, the equilibrium equations are:

$$N' + p_x = 0, \quad T' + p_y = 0, \quad M' + T + c = 0, \quad (2)$$

where $N(s, t)$, $T(s, t)$ are the axial and shear internal forces, respectively, $M(s, t)$ the bending moment, $p_x(s, t)$, $p_y(s, t)$, $c(s, t)$ are the external forces and couple per unit-length.

A linear hyperelastic law is introduced, by postulating a complete quadratic polynomial expression for the elastic potential energy density, i.e.:

$$\phi(\varepsilon, \gamma, \kappa) = \frac{1}{2} [C_{11} \varepsilon^2 + C_{22} \gamma^2 + C_{33} \kappa^2 + 2(C_{12} \varepsilon \gamma + C_{13} \varepsilon \kappa + C_{23} \gamma \kappa)]. \quad (3)$$

It leads, via the Green law, to a fully-coupled constitutive law, containing six constants C_{ij} . These latter must be properly identified, in order the Timoshenko beam model captures the macroscopic behavior of the frame. The best way consists in equating the elastic energy of the cell and that of a segment of equal length of the beam, when they undergo the same deformations, suitably chosen. In the simplest case of rigid-floors, the constants can be analytically evaluated (see [26, 18, 19, 20, 23] for details), and they assume the expressions reported in the Appendix A. If, however, the warping of the floor has to be accounted, an analytical expression can be pursued only in the special case of regular cell (i.e. with equal spans b_i and equal beam and columns, see [26]). For general geometry, a numerical approach must be followed, as explained in the next Section.



By combining kinematics, equilibrium and the elastic law, and introducing inertia forces according to the d'Alembert principle, the following equations of motions are derived:

$$\begin{aligned}
 &-\rho A \ddot{u} + I_y \ddot{\theta} + C_{11} u'' + C_{12} (v'' - \theta') + C_{13} \theta'' + p_x = 0, \\
 &-\rho A \ddot{v} + C_{12} u'' + C_{22} (v'' - \theta') + C_{23} \theta'' + p_y = 0, \\
 &-I_{yy} \ddot{\theta} + I_y \ddot{u} + C_{13} u'' + C_{23} (v'' - \theta') + C_{33} \theta'' + C_{12} u' + C_{22} (v' - \theta) + C_{23} \theta' + c = 0,
 \end{aligned}
 \tag{4}$$

where ρA , I_y , I_{yy} are the mass, first and second inertia moments per unit-length, evaluated with respect to the centroid, and a dot denotes time-differentiation. Equations (4) generalize to the dynamic case the equations obtained in [26]. The problem is complemented with the geometric boundary conditions at the ground A :

$$u_A = v_A = \theta_A = 0, \tag{5}$$

and the mechanical boundary conditions at the free end B :

$$\begin{aligned}
 C_{11} u'_B + C_{12} (v'_B - \theta_B) + C_{13} \theta'_B &= P_x, \\
 C_{12} u'_B + C_{22} (v'_B - \theta_B) + C_{23} \theta'_B &= P_y, \\
 C_{13} u'_B + C_{23} (v'_B - \theta_B) + C_{33} \theta'_B &= C,
 \end{aligned}
 \tag{6}$$

where P_x , P_y and C are point-forces and couple, and no lumped masses are present. Initial conditions, prescribing that the system is initially at rest, are also assumed.

The field equations (4), together with the boundary conditions (5) and (6) are a system of partial differential equations, which can be recast in the following matrix form:

$$\begin{aligned}
 &-\mathbf{M} \ddot{\mathbf{u}} + \mathbf{K}_2 \mathbf{u}'' + \mathbf{K}_1 \mathbf{u}' + \mathbf{K}_0 \mathbf{u} + \mathbf{p} = \mathbf{0}, \\
 &\mathbf{u}_A = \mathbf{0}, \\
 &\mathbf{K}_{1B} \mathbf{u}'_B + \mathbf{K}_{0B} \mathbf{u}_B = \mathbf{P},
 \end{aligned}
 \tag{7}$$

where:

$$\begin{aligned}
 \mathbf{u} &:= \begin{pmatrix} u \\ v \\ \theta \end{pmatrix}, & \mathbf{p} &:= \begin{pmatrix} p_x \\ p_y \\ c \end{pmatrix}, & \mathbf{P} &:= \begin{pmatrix} P_x \\ P_y \\ C \end{pmatrix}, \\
 \mathbf{M} &:= \begin{pmatrix} \rho A & 0 & -I_y \\ 0 & \rho A & 0 \\ -I_y & 0 & I_{yy} \end{pmatrix}, & \mathbf{K}_0 &:= \begin{pmatrix} 0 & 0 & 0 \\ 0 & 0 & 0 \\ 0 & 0 & -C_{22} \end{pmatrix}, & \mathbf{K}_1 &:= \begin{pmatrix} 0 & 0 & -C_{12} \\ 0 & 0 & -C_{22} \\ C_{12} & C_{22} & 0 \end{pmatrix}, \\
 \mathbf{K}_2 &:= \begin{pmatrix} C_{11} & C_{12} & C_{13} \\ C_{12} & C_{22} & C_{23} \\ C_{13} & C_{23} & C_{33} \end{pmatrix}, & \mathbf{K}_{0B} &:= \begin{pmatrix} 0 & 0 & -C_{12} \\ 0 & 0 & -C_{22} \\ 0 & 0 & -C_{23} \end{pmatrix}, & \mathbf{K}_{1B} &:= \mathbf{K}_2.
 \end{aligned}
 \tag{8}$$

Here, \mathbf{u} , \mathbf{p} , \mathbf{P} are displacement and load vectors; \mathbf{M} is the mass matrix; \mathbf{K}_j ($j = 0, \dots, 2$) are stiffness matrices; the index B denotes evaluation at the free end. Equations (7) admit a closed-form solution in statics (i.e., by disregarding the inertial effects). In dynamics, they also can be solved analytically when particular symmetries hold in the columns' layout, namely when the equations reduce to the classical (partially uncoupled) equations of the Timoshenko model [42, 43]. In the remaining cases, a numerical approach must be followed. Here, (i) the analytical solution for the static problem, and, (ii) the Finite Difference solution for the dynamic eigenvalue problem, are discussed for general frames.

3. Identification of the elastic and inertial constants

The elastic and inertial constants of the equivalent beam model are now identified by relaxing the classical rigid-floor assumption for the frame. A simpler, but approximate, analytical expression for the elastic properties is also recalled from [26].

3.1 Numerical identification of the elastic constants

The identification is carried out by equating the elastic energy stored by a cell of dimensions $b \times h$ (Fig. 2-a) and the elastic energy of a segment of Timoshenko beam, occupying the same volume (Fig. 2-b). The cell (possibly including braces) is delimited by the two horizontal floors, which are considered to have half of their stiffnesses, and restrained at the columns-floor joints by external hinges; the segment of beam is clamped at the ground. The energy equality is enforced by assigning, in the two models, the same displacements \bar{u}_i, \bar{v}_i at the points at abscissas $y = y_i$ ($i = 1, 2, \dots, m$), at which the joints are located. The rotations of joints, instead, are left free. Thus, while all the points of the rigid cross-section of the beam remain aligned in the current configuration, only the joints of the cell lie on the same line; all the remaining points of the floor depart from this line, to describe warping. Deflections of the heads of the columns are kinematically compatible with those of the floor at joints.

A uniform state of strain $\varepsilon = \text{const}$, $\gamma = \text{const}$, $\kappa = \text{const}$ is assigned to the segment of beam, and the displacements of the centroid G of the upper cross-section are determined by integration of the strain-displacement relationships (1), i.e.:

$$u_G = \varepsilon h, \quad v_G = \gamma h + \kappa \frac{h^2}{2}, \quad \theta = \kappa h. \tag{9}$$

From these latter, by using kinematics, the displacements at the abscissas y_i of the rigid cross-section are evaluated as:

$$\bar{u}_i = u_G - \theta y_i, \quad \bar{v}_i = v_G, \tag{10}$$

which, therefore, linearly depend on the strains. By enforcing these displacements at the joints of the cell, the relevant elastic problem is solved, and, in particular, the reactions r_{xi}, r_{yi} at the constraints are evaluated. Although this step could, in principle,



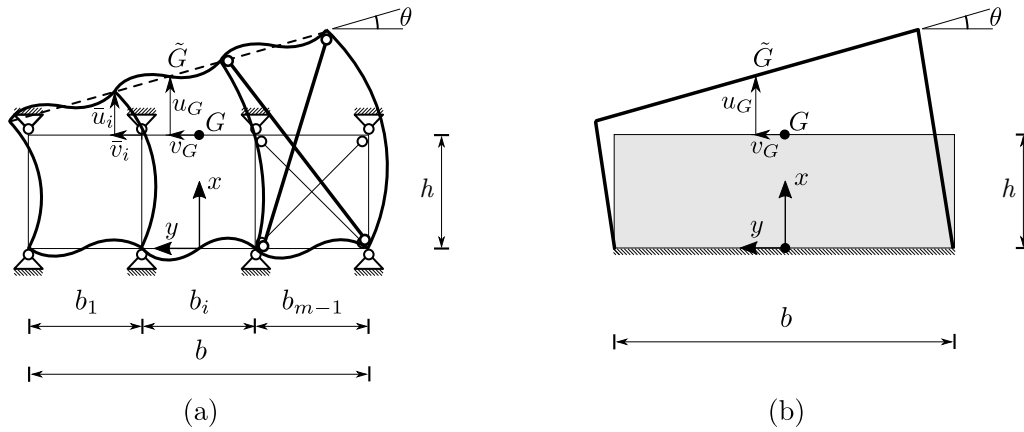


Fig. 2. Correspondence between displacements of: (a) the cell of the frame, and, (b) a segment of the Timoshenko beam.

be performed analytically, a Finite Element (FE) analysis of the cell is more convenient, from which the numerical character of the algorithm.

Finally, the elastic energy of the two models are computed: (i) the energy stored by the segment of beam is evaluated as $U_b = \phi h$, with ϕ given by Eq (3); (ii) the energy stored by the cell is determined according to the Clapeyron's theorem, as:

$$U_c = \frac{1}{2} \sum_{i=1}^m (r_{xi} \bar{u}_i + r_{yi} \bar{v}_i). \tag{11}$$

Since both the reactions and the displacements are linear functions of the strains, U_c is a homogeneous quadratic functions of these variables, like U_b . By requiring that $U_c = U_b$ for any $\varepsilon, \gamma, \kappa$, the unknown elastic constants are evaluated. However, since the assigned strains are three and the unknown constants are six, suitable combinations of the strains must be chosen, and enforced in an ordered sequence, namely: (i) just one strain at time is assigned, to evaluate C_{11}, C_{22}, C_{33} (in order for just one term in Eq (3) is different from zero); (ii) just a couple of strains at time is assigned, to compute C_{12}, C_{13}, C_{23} (in order just three terms in Eq (3) are different from zero, two of which, however, have already been determined at step (i)).

From a computational point of view, it is more convenient to assign unitary displacements and/or rotation at the joints of the floor, and to express the associated strains. Accordingly, the following algorithm is applied (Fig. 3):

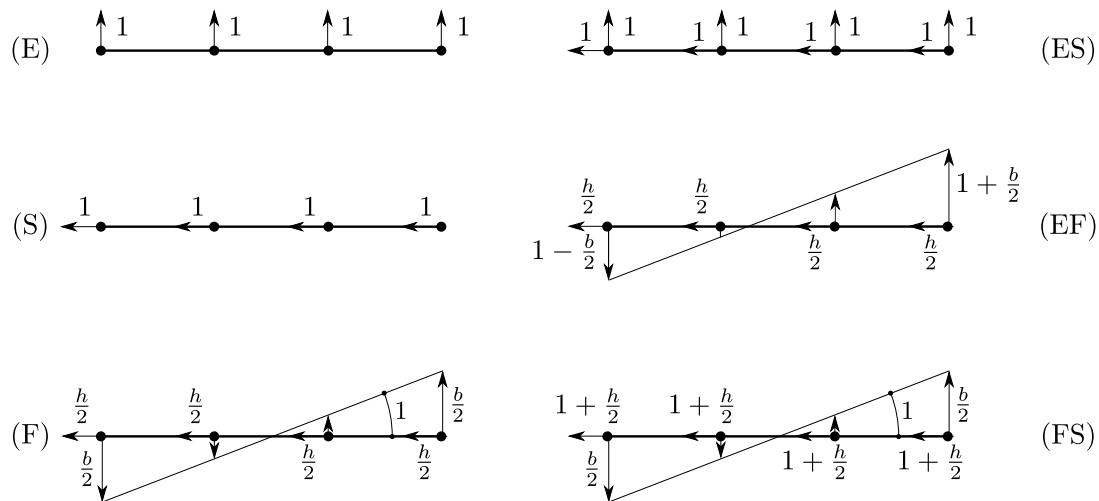


Fig. 3. Deformation modes assigned to the periodic cell: (E) extensional; (S) shear; (F) flexural; (ES) extensional plus shear; (EF) extensional plus flexural; (FS) flexural plus shear.

1. An extensional mode (E) is assigned, in which $\bar{u}_i = 1$ ($i = 1, 2, \dots, m$); since $u_G = 1, v_G = 0, \theta = 0$, then $\varepsilon = 1/h, \gamma = 0, \kappa = 0$; C_{11} is computed.
2. A shear mode (S) is assigned, in which $\bar{v}_i = 1$ ($i = 1, 2, \dots, m$); since $u_G = 0, v_G = 1, \theta = 0$, then $\varepsilon = 0, \gamma = 1/h, \kappa = 0$; C_{22} is computed.
3. A flexural mode (F) is assigned, in which $\bar{u}_i = -y_i$ ($i = 1, 2, \dots, m$), together with $\bar{v}_i = h/2$ ($i = 1, 2, \dots, m$); since $u_G = 0, v_G = h/2, \theta = 1$, then $\varepsilon = 0, \gamma = 0, \kappa = 1/h$; C_{33} is computed.
4. An extensional plus shear mode (ES), obtained by superimposing the elementary modes (E), (S), is assigned, for which $\varepsilon = 1/h, \gamma = 1/h, \kappa = 0$; since C_{11}, C_{22} are known, C_{12} is computed.



5. An extensional plus flexural mode (EF), obtained by superimposing the elementary modes (E), (F), is assigned, for which $\varepsilon = 1/h, \gamma = 0, \kappa = 1/h$; since C_{11}, C_{33} are known, C_{13} is computed.
6. A flexural plus shear mode (FS), obtained by superimposing the elementary modes (F), (S), is assigned, for which $\varepsilon = 0, \gamma = 1/h, \kappa = 1/h$; since C_{22}, C_{33} are known, C_{23} is computed.

3.2 Analytical approximation of the elastic constants

In the special case of symmetric layout of the columns, $b_i = b/(m - 1)$, and equal columns and beams of the cell, the elastic constants C_{ij} can be analytically determined under the hypotheses the floors are inextensible, and the rotations of joints are (almost) equal in modulus (due to the periodicity). This case has been studied in [26], by also taking into account for the presence of braces. It was proved there that $C_{22} = \chi_s C_{22}^\infty$ and $C_{33} = \chi_f C_{33}^\infty$, where $C_{22}^\infty, C_{33}^\infty$ are the values assumed by the constants in the rigid-floor case (see the Appendix A) and $\chi_s < 1$ and $\chi_f < 1$ are a shear and a flexural corrective factors, accounting for warping. The shear factor assumes the following expression:

$$\chi_s = \left(\frac{\frac{(m-1)^2}{m} \eta \frac{h}{b}}{1 + \frac{(m-1)^2}{m} \eta \frac{h}{b}} + \frac{(m-1)^2}{6m} \xi \frac{h}{b} (1 + \alpha_c) \cos^3(\beta) \right) \frac{1}{1 + \frac{(m-1)^2}{6m} \xi \frac{h}{b} (1 + \alpha_c) \cos^3(\beta)}, \tag{12}$$

where: $EJ_\alpha, GA_\alpha^*, EA_\alpha$ ($\alpha = b, c$) are the flexural, shear and axial stiffnesses of the micro beams, respectively, all modeled as Timoshenko beams themselves; moreover, $\eta := \frac{EJ_b}{EJ_c} \frac{1 + \alpha_c}{1 + \alpha_b}$ is a beam-to-column stiffness ratio and $\xi := \frac{EA_{br} h^2}{EJ_c}$ is a bracing-to-column stiffness ratio (see Appendix A for the remaining definitions). On the other hand, it is shown in [26] that the flexural factor is $\chi_f \simeq 1$, with or without bracing elements.

In the general case of non-regular layout, e.g. in the presence of different columns and beams and/or different span lengths, Eq (12) is no more valid. However, it is shown in [26] that, for moderately non-symmetric layouts, when the span lengths are almost equal, the coefficients C_{22} and C_{33} can be heuristically corrected by the same factors, evaluated by mean weighted values of stiffnesses of beams and columns. These corrections are shown in [26] to give reliable results in static analyses.

3.3 Identification of the inertial properties

In order to identify the inertial properties, a cell is taken, made of a horizontal beam, half of the column below it and half of the column above it. The masses of the floor and of the column are considered to be lumped at joints, so that the kinetic energy of the cell reads:

$$\mathcal{T} = \sum_{i=1}^m \frac{1}{2} M_i (\dot{u}_i^2 + \dot{v}_i^2), \tag{13}$$

where M_i are the lumped masses, and \dot{u}_i, \dot{v}_i their translational velocities (rotatory inertia neglected). It is worth noticing that, according to Eq (10), the assumption of lumped masses renders the kinetic energy independent of warping of the floors. By making use of Eq (10), and equating \mathcal{T} to the kinetic energy of a segment of beam of length h , the following identified inertial constants are found:

$$\begin{aligned} \rho A &:= \frac{1}{h} \sum_{i=1}^m M_i, \\ I_y &:= \frac{1}{h} \sum_{i=1}^m M_i y_i, \\ I_{yy} &:= \frac{1}{h} \sum_{i=1}^m M_i y_i^2. \end{aligned} \tag{14}$$

4. Analytical and numerical analyses

The exact general solution is discussed for the static problem. A numerical, Finite Difference solution is worked out for the dynamic problem.

4.1 Statics

Analytical solutions for the static boundary value problem (7) are here derived. First, the inertial terms in Eqs (7) are ignored and the general solution of the homogeneous counterpart of equations Eq (7)-a is sought in the form:

$$\mathbf{u} = \begin{pmatrix} a_1 \\ a_2 \\ a_3 \end{pmatrix} e^{\mu s}, \tag{15}$$

with μ the characteristic exponent. Accordingly, the characteristic equation reads:

$$\mu^6 \det(\mathbf{K}_2) = 0, \tag{16}$$

with $\det(\mathbf{K}_2) = C_{11}C_{22}C_{33} + 2C_{12}C_{13}C_{23} - C_{11}C_{23}^2 - C_{22}C_{13}^2 - C_{33}C_{12}^2$. The equations admits six coincident zero roots $\mu_i = 0$ ($i = 1, \dots, 6$) and only two proper eigenvectors $\mathbf{u}_{j1}, j = 1, 2$. Each of these eigenvectors generates a Jordan chain, namely $\{\mathbf{u}_{11}, \mathbf{u}_{12}\}$, of length 2, and $\{\mathbf{u}_{21}, \mathbf{u}_{22}, \mathbf{u}_{23}, \mathbf{u}_{24}\}$, of length 4 (i.e. the state-space matrix, governing the static problem associated to Eq (7) when put in the first-order form, admits a Jordan canonical form made of two blocks, of dimension 2 and 4, respectively) [44]. The general solution, consequently, assumes the form:

$$\begin{aligned} \mathbf{u} &= c_1 \mathbf{u}_{11} + c_2 (\mathbf{u}_{11} s + \mathbf{u}_{12}) + c_3 \mathbf{u}_{21} + c_4 (\mathbf{u}_{21} s + \mathbf{u}_{22}) + c_5 \left(\mathbf{u}_{21} \frac{s^2}{2} + \mathbf{u}_{22} s + \mathbf{u}_{23} \right) \\ &+ c_6 \left(\mathbf{u}_{21} \frac{s^3}{6} + \mathbf{u}_{22} \frac{s^2}{2} + \mathbf{u}_{23} s + \mathbf{u}_{24} \right), \end{aligned} \tag{17}$$



where c_i ($i = 1, \dots, 6$) are arbitrary constants. The particular solution of the non-homogeneous Eq (7)-a is easily evaluated once the loads are specified. The constants c_i are then determined by enforcing the boundary conditions (7)-b,c.

In the special (but frequent) case in which $\mathbf{P} = \mathbf{0}$ and $\mathbf{p} = (0, p_y, 0)^T$, p_y being a constant on s , the solution to Eqs (7) is found to be:

$$\begin{aligned} u &= -\frac{p_y}{2 \det(\mathbf{K}_2)} \left\{ [(C_{13}C_{22} - C_{12}C_{23}) \ell + 2(C_{12}C_{33} - C_{13}C_{23})] \ell s \right. \\ &\quad \left. + [(C_{12}C_{23} - C_{13}C_{22}) \ell + C_{13}C_{23} - C_{12}C_{33}] s^2 + (C_{13}C_{22} - C_{12}C_{23}) \frac{s^3}{3} \right\}, \\ v &= -\frac{p_y}{2 \det(\mathbf{K}_2)} \left\{ [(C_{11}C_{23} - C_{12}C_{13}) \ell + 2(C_{13}^2 - C_{11}C_{33})] \ell s \right. \\ &\quad \left. + [(C_{12}^2 - C_{11}C_{22}) \ell^2 + 2(C_{11}C_{33} - C_{13}^2)] \frac{s^2}{2} + (C_{11}C_{22} - C_{12}^2) \ell \frac{s^3}{3} + (C_{12}^2 - C_{11}C_{22}) \frac{s^4}{12} \right\}, \\ \theta &= -\frac{p_y}{2 \det(\mathbf{K}_2)} \left\{ [(C_{12}^2 - C_{11}C_{22}) \ell + 2(C_{11}C_{23} - C_{13}C_{12})] \ell s \right. \\ &\quad \left. + [(C_{11}C_{22} - C_{12}^2) \ell + C_{13}C_{12} - C_{11}C_{23}] s^2 + (C_{12}^2 - C_{11}C_{22}) \frac{s^3}{3} \right\}. \end{aligned} \quad (18)$$

4.2 Dynamics

The dynamic eigenvalue problem is addressed. By letting $\mathbf{p} = \mathbf{P} = \mathbf{0}$ and $\mathbf{u} = \hat{\mathbf{u}}(s) e^{\lambda t}$ in Eqs (7), $(\lambda, \hat{\mathbf{u}}(s))$ being the eigenpairs of the system, the following (spatial) boundary value problem (BVP) is found:

$$\begin{aligned} \mathbf{K}_2 \hat{\mathbf{u}}'' + \mathbf{K}_1 \hat{\mathbf{u}}' + \mathbf{K}_0 \hat{\mathbf{u}} - \lambda^2 \mathbf{M} \hat{\mathbf{u}} &= \mathbf{0}, \\ \hat{\mathbf{u}}_A &= \mathbf{0}, \\ \mathbf{K}_{1B} \hat{\mathbf{u}}'_B + \mathbf{K}_{0B} \hat{\mathbf{u}}_B &= \mathbf{0}. \end{aligned} \quad (19)$$

The exact solution to these equations can still be pursued, but it calls for numerically solving the dispersion relation between the eigenvalue λ and wave-number μ . Therefore, an alternative, purely numerical approach, is followed here.

Equations (22) are discretized via the Finite Difference Method. Accordingly, the domain $[0, \ell]$ is divided in L elements and $L + 1$ nodes of coordinates $s_i = i \Delta$ ($i = 0, 1, \dots, L$), with $\Delta := \ell/L$. A dummy node $L + 1$ is added, of coordinates $s_{L+1} = (L + 1) \Delta$. By using central finite differences, the derivatives are approximated as follows:

$$\begin{aligned} \hat{\mathbf{u}}_i &= \hat{\mathbf{u}}(s_i), \\ \hat{\mathbf{u}}'_i &= \frac{\hat{\mathbf{u}}_{i+1} - \hat{\mathbf{u}}_{i-1}}{2 \Delta}, \\ \hat{\mathbf{u}}''_i &= \frac{\hat{\mathbf{u}}_{i+1} - 2\hat{\mathbf{u}}_i + \hat{\mathbf{u}}_{i-1}}{\Delta^2}. \end{aligned} \quad (20)$$

Thus, the BVP (19) is transformed into an algebraic problem:

$$\begin{aligned} \hat{\mathbf{u}}_0 &= \mathbf{0}, \\ \left(\frac{1}{\Delta^2} \mathbf{K}_2 - \frac{1}{2\Delta} \mathbf{K}_1 \right) \hat{\mathbf{u}}_{i-1} + \left(\mathbf{K}_0 - \frac{2}{\Delta^2} \mathbf{K}_2 \right) \hat{\mathbf{u}}_i + \left(\frac{1}{\Delta^2} \mathbf{K}_2 + \frac{1}{2\Delta} \mathbf{K}_1 \right) \hat{\mathbf{u}}_{i+1} - \lambda^2 \mathbf{M} \hat{\mathbf{u}}_i &= \mathbf{0}, \quad i = 1, \dots, L, \\ -\frac{1}{2\Delta} \mathbf{K}_{1B} \hat{\mathbf{u}}_{L-1} + \mathbf{K}_{0B} \hat{\mathbf{u}}_L + \frac{1}{2\Delta} \mathbf{K}_{1B} \hat{\mathbf{u}}_{L+1} &= \mathbf{0}, \end{aligned} \quad (21)$$

or, in compact form:

$$(\mathbf{K} - \lambda^2 \mathbf{M}) \mathbf{u} = \mathbf{0}, \quad (22)$$

where $\mathbf{u} = (\hat{\mathbf{u}}_0, \dots, \hat{\mathbf{u}}_L, \hat{\mathbf{u}}_{L+1})^T$, \mathbf{K} and \mathbf{M} are the (discrete) stiffness and mass matrices, having dimension $3(L + 2) \times 3(L + 2)$. Equation (22) is the discrete counterpart of the BVP (19). It is solved by standard numerical algorithms.

5. Numerical results

Numerical results are referred to three planar frames, made of concrete and steel, shown in Fig. 4. They are analyzed in statics, under lateral loads, and in free dynamics, by accounting for self-mass. They are clamped at the ground, made of four spans (whose lengths are reported in the same figure) and $n = 25$ floors, with inter-floor height $h = 4$ m; moreover, they are statically loaded by horizontal point forces at each floor, $F = 50$ kN (see Fig. 4). The detailed description of the case studies is reported in the following.

- Case study I: symmetric concrete frame, displayed in Fig. 4-a, having elastic modulus $E = 3 \times 10^7$ kN/m², Poisson coefficient $\nu = 0.2$ and mass density $\rho = 2500$ kg/m³. The beams' cross-section is rectangular, of dimensions 0.4 m \times 1.0 m; the columns' cross-section is also rectangular, of dimensions 0.7 m \times 0.7 m.
- Case study II: not-symmetric concrete frame, displayed in Fig. 4-b, having elastic modulus $E = 3 \times 10^7$ kN/m², Poisson coefficient $\nu = 0.2$ and mass density $\rho = 2500$ kg/m³. Beams' and columns' cross-sections are rectangular, and labeled in Fig. 4-b.
- Case study III: slightly not-symmetric steel braced frame, displayed in Fig. 4-c, having elastic modulus $E = 2 \times 10^8$ kN/m², Poisson coefficient $\nu = 0.3$ and mass density $\rho = 7850$ kg/m³. Beams', columns' and bracings' cross-sections are (commercial nomenclature) HEA 450, HEA 600, SHS 100×10 , respectively.

The geometric properties of the cross-sections are reported in Tab. 1 (A is the area, A^* the shear area, J the inertia moment).



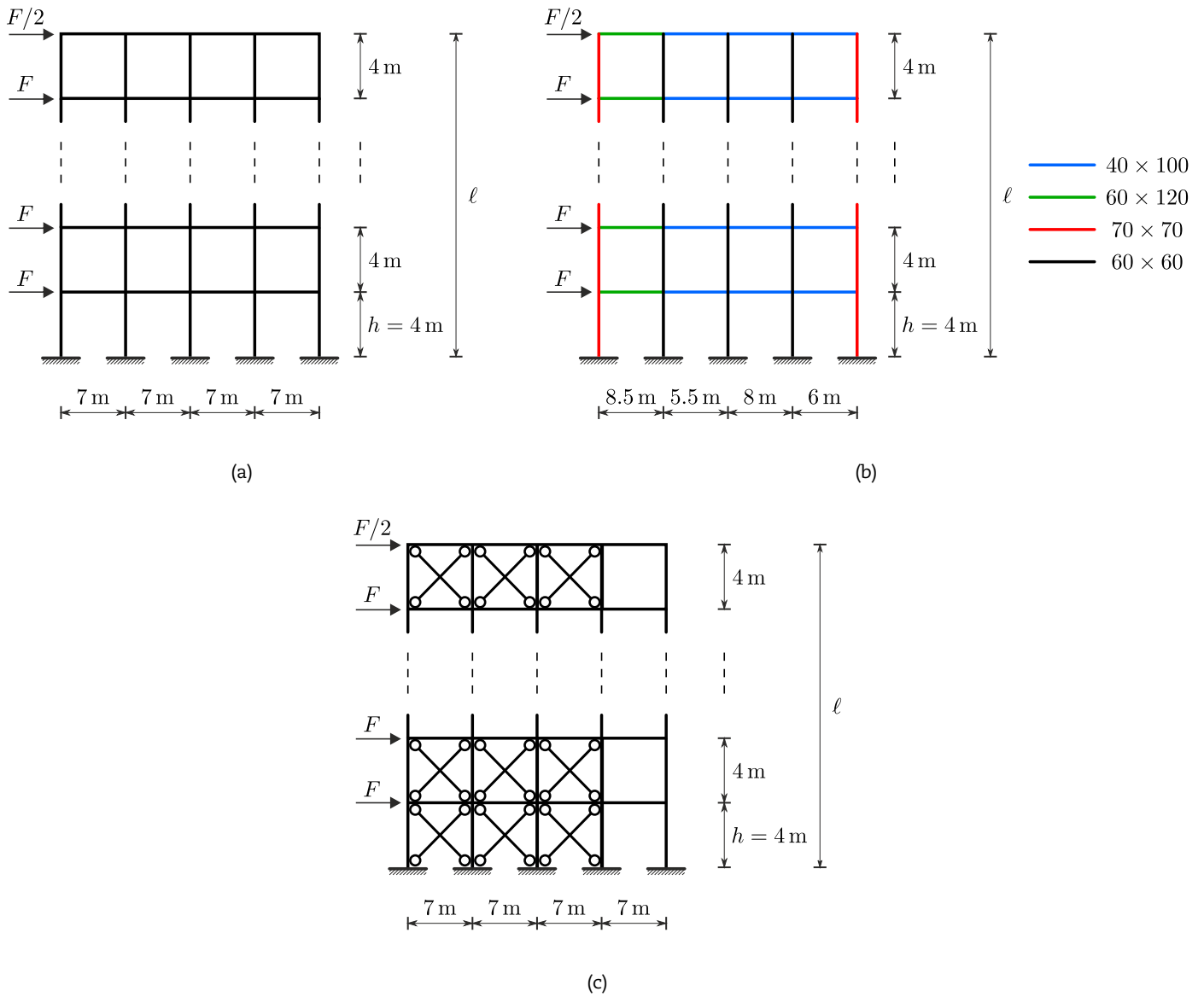


Fig. 4. Planar frames under horizontal loads: (a) case study I; (b) case study II; (c) case study III.

Case study	Type	Name	A [m ²]	A^* [m ²]	J [m ⁴]
I, II	beam	0.4 m × 1.0 m	0.4	0.33	3.33×10^{-2}
I, II	column	0.7 m × 0.7 m	0.49	0.41	2.0×10^{-2}
II	beam	0.6 m × 1.2 m	0.72	0.6	8.64×10^{-2}
II	column	0.6 m × 0.6 m	0.36	0.3	1.08×10^{-2}
III	beam	HEA 450	1.72×10^{-2}	1.05×10^{-2}	6.14×10^{-4}
III	bracing	SHS 100 × 10	3.60×10^{-3}	2.00×10^{-3}	4.92×10^{-6}
III	column	HEA 600	2.20×10^{-2}	1.25×10^{-2}	1.36×10^{-3}

Table 1. Cross-sections properties for the case studies I, II, III.

Elasto-geometric and inertial properties

The elasto-geometric and inertial properties of the equivalent beam models are reported in Tab. 2 for each case study. Analytical (approximate) C_{ij}^a [26] and numerical (exact) C_{ij}^n (Sect. 3.) values have been obtained for the elastic constants C_{ij} , and the percentage error $\epsilon\% = 100 (C_{ij}^n - C_{ij}^a) / C_{ij}^n$ reported in the same Table. The analytical values are based: on the shear factor concept (case I), (heuristically) averaged in non-symmetric cases (cases II, III). The shear factor only affects C_{22} , the remaining constants being independent of the floor flexibility.

It is found that the two procedures supply values which are quite close each other. In particular, the agreement is very good in the symmetric case I and in the weakly non-symmetric case III, while larger differences occur, as expected, in the strongly non-symmetric case II. Such a conclusion, however, concerns the examined frames, for which extension and bending are uncoupled from shear (entailing $C_{12} = C_{23} = 0$), as due to the fact that bracings are not present at all (cases I and II), or they are organized



Case study I				
		Analytical	Numerical	$\epsilon\%$
C_{11}	[kN]	7.350×10^7	7.350×10^7	0
C_{22}	[kN]	9.082×10^5	8.811×10^5	-3.08
C_{33}	[kN \times m ²]	7.206×10^9	7.206×10^9	0
C_{12}	[kN]	0	0	–
C_{13}	[kN \times m]	0	0	–
C_{23}	[kN \times m]	0	0	–
m	[kg/m]	1.313×10^4	–	–
I_y	[kg]	0	–	–
I_{yy}	[kg \times m]	1.115×10^6	–	–

Case study II				
		Analytical	Numerical	$\epsilon\%$
C_{11}	[kN]	6.180×10^7	6.180×10^7	0
C_{22}	[kN]	9.026×10^5	8.045×10^5	-12.20
C_{33}	[kN \times m ²]	6.782×10^9	6.782×10^9	0
C_{12}	[kN]	0	0	–
C_{13}	[kN \times m]	2.700×10^7	2.700×10^7	0
C_{23}	[kN \times m]	0	0	–
m	[kg/m]	1.385×10^4	–	–
I_y	[kg]	1.433×10^4	–	–
I_{yy}	[kg \times m]	1.278×10^6	–	–

Case study III				
		Analytical	Numerical	$\epsilon\%$
C_{11}	[kN]	2.253×10^7	2.253×10^7	0
C_{22}	[kN]	1.779×10^6	1.769×10^6	-0.60
C_{33}	[kN \times m ²]	2.181×10^9	2.181×10^9	0
C_{12}	[kN]	0	0	–
C_{13}	[kN \times m]	-1.847×10^6	-1.847×10^6	0
C_{23}	[kN \times m]	0	0	–
m	[kg/m]	2.150×10^3	–	–
I_y	[kg]	1.173×10^3	–	–
I_{yy}	[kg \times m]	1.738×10^5	–	–

Table 2. Analytical and numerical values of the elasto-geometric and mass coefficients of the equivalent beam model. The analytical C_{22} is corrected by the shear factor in Eq (12).

in a bi-directionally oriented and symmetric pattern in some spans (case III). For more general conclusion, relevant for example to frames with mono-oriented braces, further investigations would be needed.

Statics

Numerical results concern the linear static response of the frames described above. Here, the analytical solution relevant to the macro beam model (Sect 4.) is compared with numerical results obtained by microscopic FE models. Comparison is made in terms of: (i) lateral displacement of the frame $v(s)$, and (ii) vertical displacements of the floor at selected floors $s = \bar{s}$, namely $u(\bar{s}, y) = u(\bar{s}) - \theta(\bar{s})y$. The aim is to validate the effectiveness of the coarse model in reproducing the static behavior of real frames. In all the cases, the equivalent beam is loaded by a constant distributed load $p_y = -F/h = -12.5$ kN/m, for which the solution (18) holds. Results of the analysis are shown in Figs. 5, 6 and 7 for the case studies I, II and III, respectively. Sub-figures 5-a, 6-a, and 7-a are relevant to the lateral displacement, while sub-figures 5-b,c,d, 6-b,c,d, and 7-b,c,d show the vertical displacement of the floor at three different levels, namely $\bar{s} = h, 12h, \ell$, respectively. Moreover, in each figure, blue dots represent the FE solution, while the continuous red curves describe the solution of the continuous model.

A good accordance of lateral displacements is found in cases I and II (see Figs. 5-a and 6-a), for which the order of magnitude of the error, evaluated at $s = \ell$, is about 1 % (case I) and 5 % (case II). In contrast, some important quantitative differences occur in case III, where the error reaches 16 % (see Fig. 7-a). In all the cases, the vertical displacements of the FE models, at different levels, are well captured by the equivalent beam model, by remembering that the rigid cross-section represents the mean-value of the rotation of the deformable floor (see Figs. 5-b,c,d, 6-b,c,d, and 7-b,c,d).

These latter sub-figures 7-b,c,d suggest the source of the larger error occurring in case III: this is due to a localized deformation of the floor, which is caused by an abrupt change of the stiffness in the fourth span (spanning the interval $y \in (-14, -7)$), where no bracing elements are present. As a matter of fact, the blue dot at $y = -14$ is misaligned with respect to the others dots, which, in contrast, are close to a straight line. It means that the Timoshenko beam model, which averages warping by a straight line, is not sufficiently accurate when warping rapidly changes. To take into account for this effect, it would be necessary to resort to more refined beam theories, able to locally describe possible deformation modes of the cross-section, as the Generalized Beam Theory (see, e.g., [45, 46, 47]).



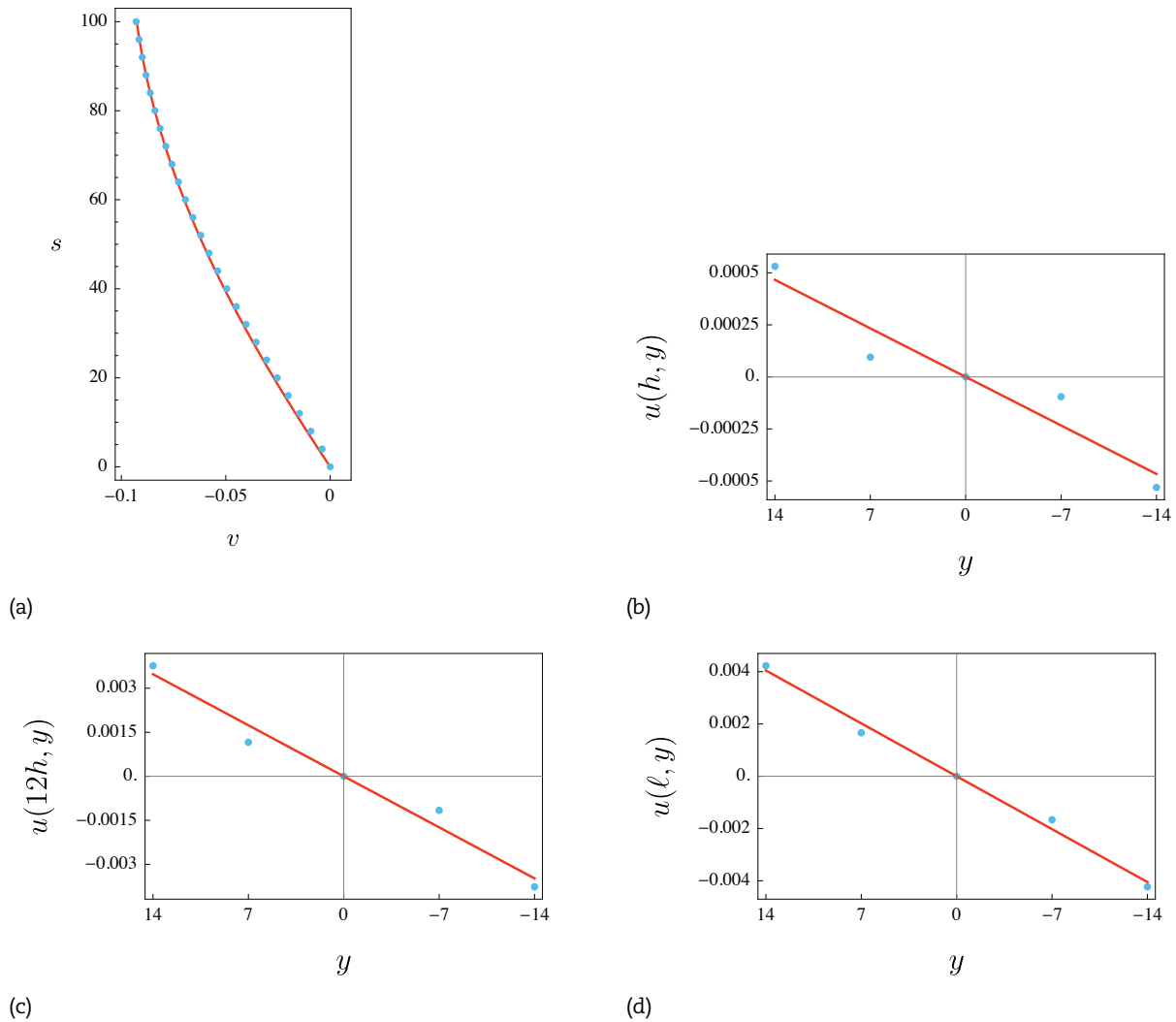


Fig. 5. Displacements of the equivalent model vs discrete FE model, for case study I: (a) lateral displacement of the frame; (b), (c), (d) vertical displacement of the floor when $\bar{s} = h, 12h, \ell$, respectively. Blue dots: discrete FE solution. Continuous red line: homogenized beam model.

Dynamics

Results of modal analysis for the three case studies are here discussed. Solutions to the eigenvalue problem of the equivalent beam model is found by using the Finite Difference (FD) method developed in Sect. 4.. These are compared with those obtained by FE results, to check the effectiveness of the homogenized beam model in capturing frequencies and modal shapes of real frames. A number of $L = 25$ nodes was taken in the FD approach, so that the system has 81 degrees of freedom, against the 375 degrees of freedom of the FE model.

Comparison, relevant to the first three modes, is presented in Tab. 3 for all the case studies. Due to conservativeness of the problem at hand, the eigenvalues are purely imaginary, namely $\lambda_j = \pm i\omega_j$, where ω_j is the angular frequencies of the j -th mode. In the Table, ω_{FE}, ω_{EQ} refer to FE and equivalent beam model solutions, respectively; moreover, $\epsilon_{\%} = 100 (\omega_{FE} - \omega_{EQ}) / \omega_{FE}$ is the percentage error. It is seen that the equivalent beam model well approximates the first three frequencies of the fine model, particularly in the case studies I and II, where the maximum error is about 4%. Otherwise, in case study III, the percentage error increases (up to about 10%), this behavior being in agreement with the results of static analysis.

An excellent correspondence between the modal shapes of the first three modes is detected in case studies I and II (see Figs. 8 and 9), where the the lateral displacements furnished by the FE solution (blue dots) are almost superimposed to the analytical ones (continuous red curves). Finally, in the case study III, the accuracy of the equivalent model is worsen just in the third mode.

6. Conclusions

A one-dimensional Timoshenko beam model, embedded in a bi-dimensional space, able to capture the overall behavior of planar frames, both in statics and dynamics, has been formulated. The equivalent model has been derived by a direct approach, concerning kinematics and static aspects, and by a homogenization method, concerning the constitutive law. The elastic constants have been determined by enforcing an energy equivalence between the cell of the periodic frame and a segment of the equivalent beam, undergoing the same generalized strains.

Differently from frames of simple geometry, for which analytical solutions (provided in [26]) are available, here a numerical identification algorithm, grounded on a FE analysis of the cell, has been presented for periodic frames with general properties. However, analytical expressions for the inertial properties of the equivalent model have still been found, under the simplifying assumption that the masses are lumped at the joints. Closed-form solutions have been worked out for the static boundary value problem, and a Finite Difference algorithm for the dynamic eigenvalue problem has been implemented.



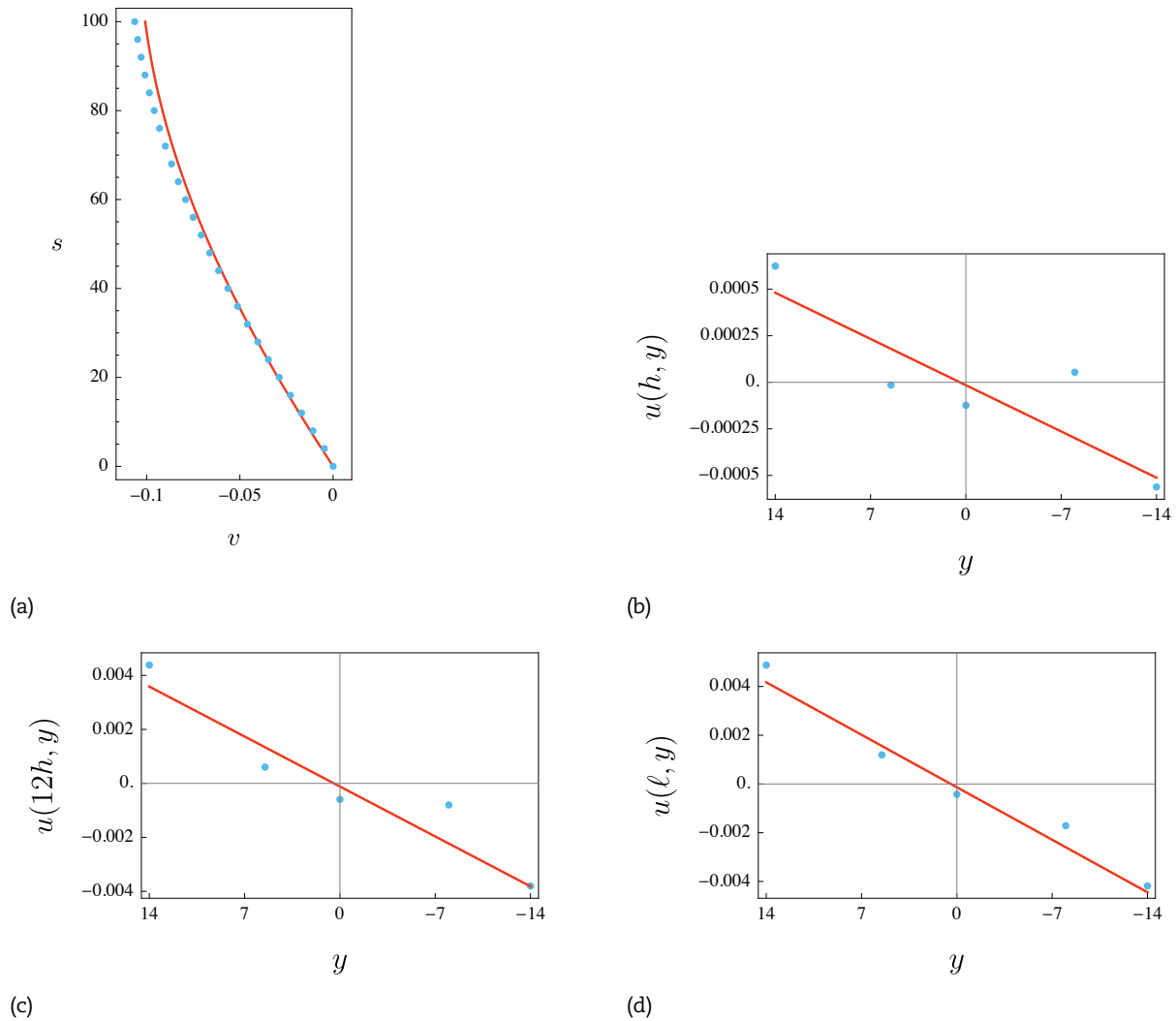


Fig. 6. Displacements of the equivalent model vs discrete FE model, for case study II: (a) lateral displacement of the frame; (b), (c), (d) vertical displacement of the floor when $\bar{s} = h, 12h, \ell$, respectively. Blue dots: discrete FE solution. Continuous red line: homogenized beam model.

Case study	Mode	ω_{FE} [rad]	ω_{EQ} [rad]	$\epsilon\%$ [-]
I	1	3.62	3.67	-1.34
	2	11.14	11.18	-0.36
	3	19.95	19.88	0.32
II	1	3.29	3.42	-4.03
	2	10.15	10.42	-2.65
	3	18.21	18.48	-1.47
III	1	7.98	8.82	-10.53
	2	29.36	31.42	-7.00
	3	49.87	50.67	-1.61

Table 3. Angular frequencies of the first three modes for all the case studies: ω_{FE}, ω_{EQ} refer to FE and equivalent beam model solutions, respectively.

The limits of applicability of the homogenized beam models have been discussed with reference to sample frames, for which the static response and modal properties have been computed. Comparisons with Finite Element analyses have been carried out to validate the model.

The following conclusions are drawn.

1. The equivalent beam model, with identified elastic and inertial constants, is able to describe the behavior of planar frames, both in statics and in dynamics.
2. A good agreement between the constitutive coefficients, evaluated by analytical and numerical procedures, is detected.
3. The equivalent beam model, in statics, supplies lateral and vertical displacements which are in excellent agreement with exact Finite Element analyses. Some differences arise when localized deformations of the floor manifest themselves, caused by the strong stiffness variability in the cell, calling for more refined beam models, to be developed.



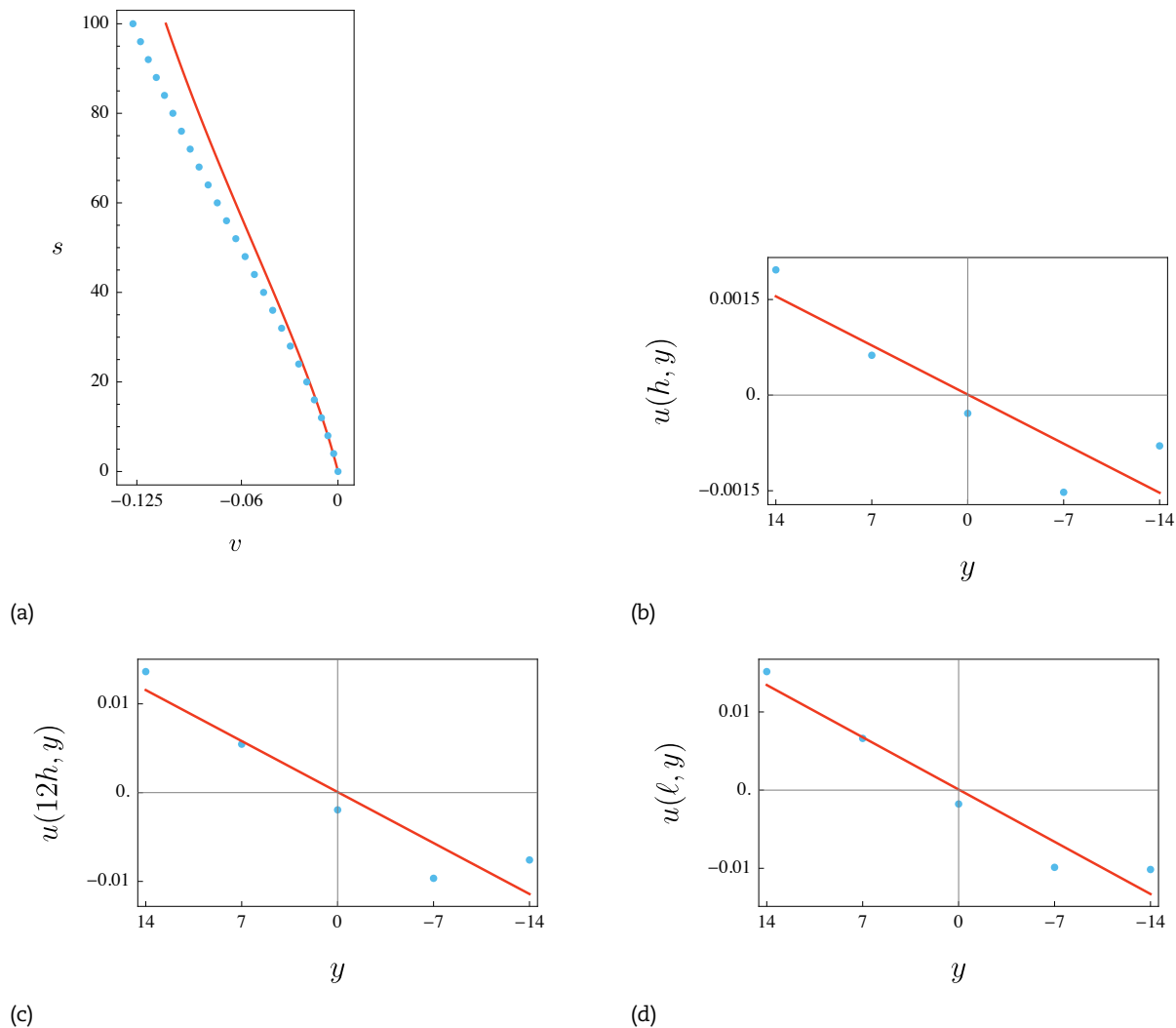


Fig. 7. Displacements of the equivalent model vs discrete FE model, for case study III: (a) lateral displacement of the frame; (b), (c), (d) vertical displacement of the floor when $\bar{s} = h, 12h, \ell$, respectively. Blue dots: discrete FE solution. Continuous red line: homogenized beam model.

4. The equivalent beam model, in dynamics, also gives very satisfactory results in terms of natural frequencies and modes. Also in this case, the occurrence of localized deformation of the cell floor, induced by jumps of stiffness, worsens the accuracy.

Author Contributions

All authors contributed equally to this work. Angelo Luongo conceived the scientific idea of this paper. Manuel Ferretti and Francesco D'Annibale developed analytical solutions and carried out numerical simulations. The manuscript was written through the contribution of all authors. All authors discussed the results, reviewed and approved the final version of the manuscript.

Conflict of Interest

The authors declared no potential conflicts of interest with respect to the research, authorship and publication of this article.

Funding

The authors received no financial support for the research, authorship and publication of this article.

References

- [1] Noor, A.K., Continuum modeling for repetitive lattice structures, *Applied Mechanics Reviews*, 1988, 41(7), 285–296.
- [2] Tollenaere, H., Caillerie, D., Continuous modeling of lattice structures by homogenization, *Advances in Engineering Software*, 1998, 29(7), 699 – 705.
- [3] Boutin, C., dell'Isola, F., Giorgio, I., Placidi, L., Linear pantographic sheets: Asymptotic micro-macro models identification, *Mathematics and Mechanics of Complex Systems*, 2017, 5(2), 127–162.
- [4] dell'Isola, F., Eremeyev, V.A., Porubov, A., *Advances in Mechanics of Microstructured Media and Structures*, vol. 87, Springer, 2018.
- [5] Di Nino, S., Luongo, A., A simple homogenized orthotropic model for in-plane analysis of regular masonry walls, *International Journal of Solids and Structures*, 2019, 167, 156–169.
- [6] Boutin, C., Hans, S., Chesnais, C., *Generalized Beams and Continua. Dynamics of Reticulated Structures*, Springer New York, New York, NY, 2010, 131–141.
- [7] dell'Isola, F., Seppecher, P., Spagnuolo, M., et al., Advances in pantographic structures: design, manufacturing, models, experiments and image analyses, *Continuum Mechanics and Thermodynamics*, 2019, 31(4), 1231–1282.



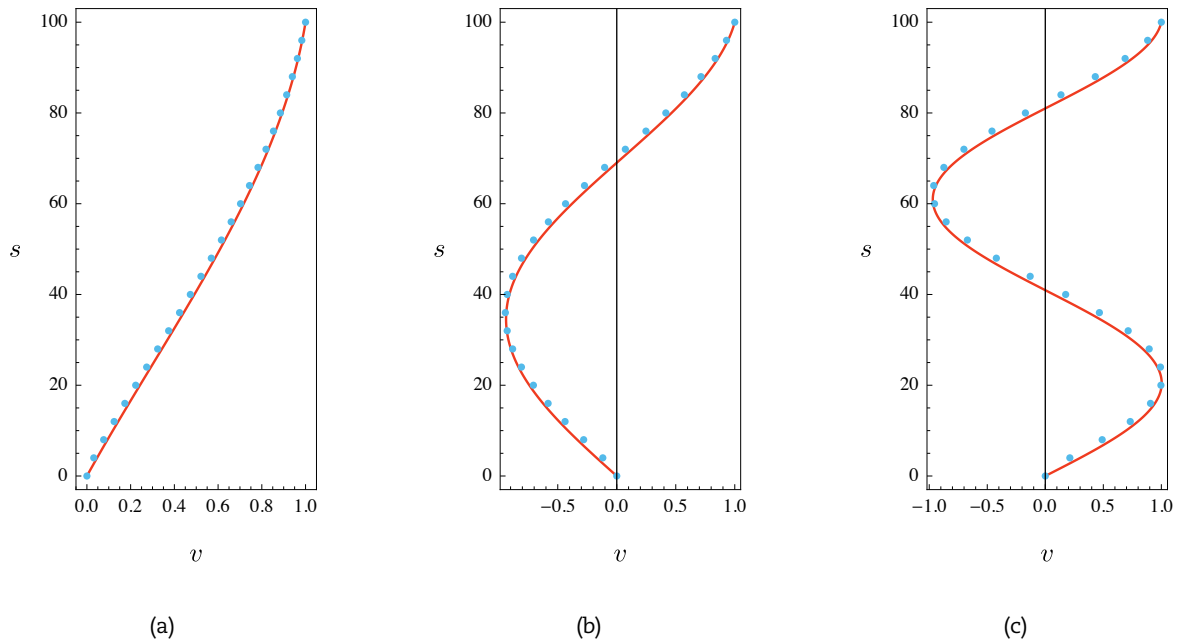


Fig. 8. Lateral displacement of the first three modes of the equivalent model vs discrete FE model, for case study I: (a) first; (b) second; (c) third. Blue dots: discrete FE solution. Continuous red line: homogenized beam model.

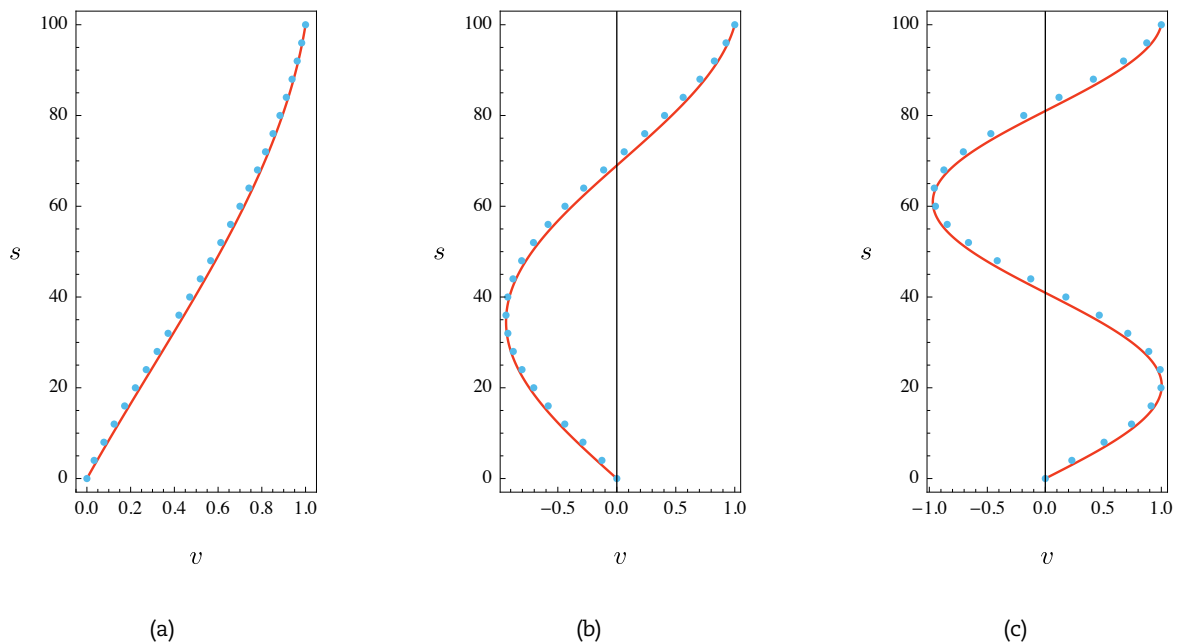


Fig. 9. Lateral displacement of the first three modes of the equivalent model vs discrete FE model, for case study II: (a) first; (b) second; (c) third. Blue dots: discrete FE solution. Continuous red line: homogenized beam model.

[8] dell’Isola, F., Seppecher, P., Alibert, J.J., et al., Pantographic metamaterials: an example of mathematically driven design and of its technological challenges, *Continuum Mechanics and Thermodynamics*, 2019, 31(4), 851–884.

[9] De Angelo, M., Barchiesi, E., Giorgio, I., Abali, B.E., Numerical identification of constitutive parameters in reduced-order bi-dimensional models for pantographic structures: application to out-of-plane buckling, *Archive of Applied Mechanics*, 2019, 89(7), 1333–1358.

[10] Giorgio, I., Rizzi, N.L., Turco, E., Continuum modelling of pantographic sheets for out-of-plane bifurcation and vibrational analysis, *Proceedings of the Royal Society A: Mathematical, Physical and Engineering Sciences*, 2017, 473(2207), 20170636.

[11] Boutin, C., Hans, S., Homogenisation of periodic discrete medium: Application to dynamics of framed structures, *Computers and Geotechnics*, 2003, 30(4), 303–320.

[12] Chajes, M.J., Romstad, K.M., McCallen, D.B., Analysis of multiple-bay frames using continuum model, *Journal of Structural Engineering*, 1993, 119(2), 522–546.

[13] Chajes, M.J., Finch, W.W., Kirby, J.T., Dynamic analysis of a ten-story reinforced concrete building using a continuum model, *Computers & structures*, 1996, 58(3), 487–498.

[14] Chajes, M.J., Zhang, L., Kirby, J.T., Dynamic analysis of tall building using reduced-order continuum model, *Journal of Structural Engineering*, 1996, 122(11), 1284–1291.

[15] Hans, S., Boutin, C., Dynamics of discrete framed structures: A unified homogenized description, *Journal of Mechanics of Materials and Structures*, 2008, 3(9), 1709–1739.

[16] Chesnais, C., Boutin, C., Hans, S., *Structural Dynamics and Generalized Continua*, Springer Berlin Heidelberg, Berlin, Heidelberg, 2011, 57–76.



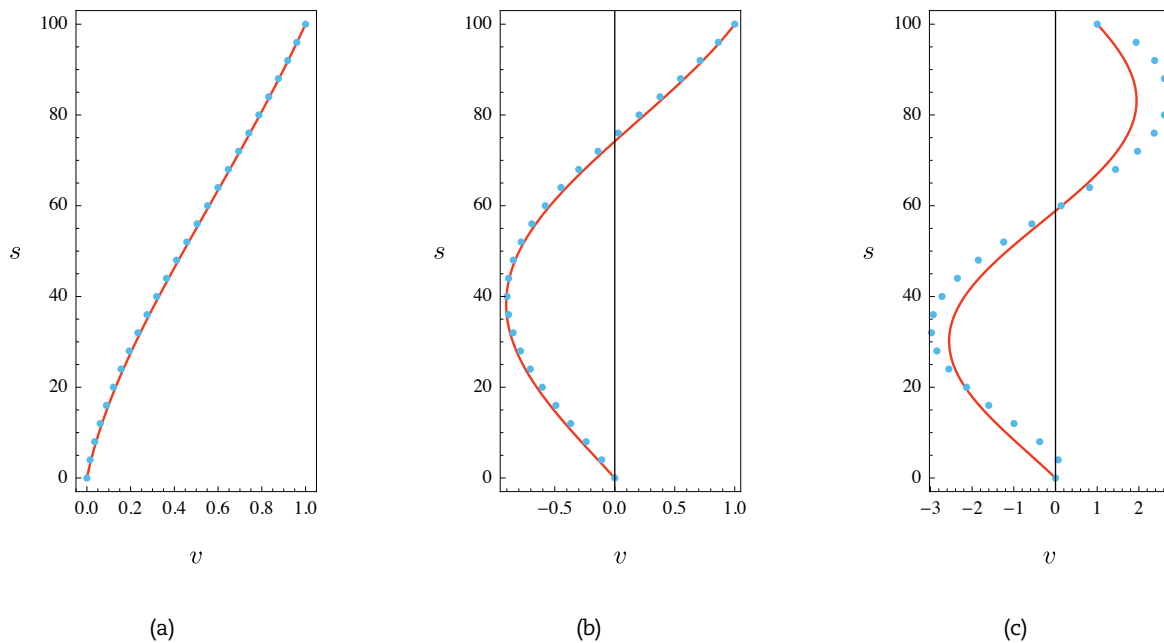


Fig. 10. Lateral displacement of the first three modes of the equivalent model vs discrete FE model, for case study III: (a) first; (b) second; (c) third. Blue dots: discrete FE solution. Continuous red line: homogenized beam model.

- [17] Cluni, F., Giofrè, M., Gusella, V., Dynamic response of tall buildings to wind loads by reduced order equivalent shear-beam models, *Journal of Wind Engineering and Industrial Aerodynamics*, 2013, 123, 339–348.
- [18] Piccardo, G., Tubino, F., Luongo, A., A shear–shear torsional beam model for nonlinear aeroelastic analysis of tower buildings, *Zeitschrift für angewandte Mathematik und Physik*, 2015, 66(4), 1895–1913.
- [19] Piccardo, G., Tubino, F., Luongo, A., Equivalent nonlinear beam model for the 3-d analysis of shear-type buildings: Application to aeroelastic instability, *International Journal of Non-Linear Mechanics*, 2016, 80, 52–65.
- [20] Piccardo, G., Tubino, F., Luongo, A., Equivalent timoshenko linear beam model for the static and dynamic analysis of tower buildings, *Applied Mathematical Modelling*, 2019, 71, 77–95.
- [21] Potzta, G., Kollár, L., Analysis of building structures by replacement sandwich beams, *International Journal of Solids and Structures*, 2003, 40(3), 535–553.
- [22] Zalka, K.A., *Global structural analysis of buildings*, CRC Press, 2002.
- [23] D’Annibale, F., Ferretti, M., Luongo, A., Shear-shear-torsional homogenous beam models for nonlinear periodic beam-like structures, *Engineering Structures*, 2019, 184, 115–133.
- [24] Di Nino, S., Luongo, A., Nonlinear aeroelastic behavior of a base-isolated beam under steady wind flow, *International Journal of Non-Linear Mechanics*, 2020, 119, 103340.
- [25] Luongo, A., Zulli, D., Free and forced linear dynamics of a homogeneous model for beam-like structures, *Meccanica*, 2019, 1–19.
- [26] Luongo, A., D’Annibale, F., Ferretti, M., Shear and flexural factors for homogenized beam models of planar frames, *Submitted to Engineering Structures*, 2020.
- [27] Bui, Q.B., Hans, S., Boutin, C., Dynamic behaviour of an asymmetric building: experimental and numerical studies, *Case Studies in Nondestructive Testing and Evaluation*, 2014, 2, 38–48.
- [28] Kim, H.S., Lee, D.G., Kim, C.K., Efficient three-dimensional seismic analysis of a high-rise building structure with shear walls, *Engineering structures*, 2005, 27(6), 963–976.
- [29] Liu, H., Yang, Z., Gaulke, M.S., Structural identification and finite element modeling of a 14-story office building using recorded data, *Engineering Structures*, 2005, 27(3), 463–473.
- [30] Sun, C.T., Kim, B.J., Bogdanoff, J.L., On the derivation of equivalent simple models for beam- and plate-like structures in dynamic analysis, *Dynamics Specialists Conference*, 624.
- [31] Zalka, K.A., A simplified method for calculation of the natural frequencies of wall-frame buildings, *Engineering Structures*, 2001, 23(12), 1544–1555.
- [32] Zalka, K., A simple method for the deflection analysis of tall wall-frame building structures under horizontal load, *The Structural Design of Tall and Special Buildings*, 2009, 18(3), 291–311.
- [33] Nassar, H., He, Q.C., Auffray, N., On asymptotic elastodynamic homogenization approaches for periodic media, *Journal of the Mechanics and Physics of Solids*, 2016, 88, 274–290.
- [34] Ferretti, M., Flexural torsional buckling of uniformly compressed beam-like structures, *Continuum Mechanics and Thermodynamics*, 2018, 30(5), 977–993.
- [35] Ferretti, M., D’Annibale, F., Luongo, A., Buckling of tower-buildings on elastic foundation under compressive tip-forces and self-weight, *Submitted to Continuum Mechanics and Thermodynamics*, 2020.
- [36] Antman, S.S., *The theory of rods, Linear Theories of Elasticity and Thermoelasticity*, Springer, 1973, 641–703.
- [37] Antman, S.S., *Nonlinear problems of elasticity*, Springer-Verlag, 2005.
- [38] Capriz, G., A contribution to the theory of rods, *Riv. Mat. Univ. Parma*, 1981, 7(4), 489–506.
- [39] Luongo, A., Zulli, D., *Mathematical models of beams and cables*, John Wiley & Sons, 2013.
- [40] Altenbach, H., Birsan, M., Eremeyev, V.A., *Cosserat-type rods, Generalized Continua from the Theory to Engineering Applications*, Springer, 2013, 179–248.
- [41] Steigmann, D.J., Faulkner, M.G., Variational theory for spatial rods, *Journal of Elasticity*, 1993, 33(1), 1–26.
- [42] Cazzani, A., Stochino, F., Turco, E., On the whole spectrum of timoshenko beams. part i: a theoretical revisitation, *Zeitschrift für angewandte Mathematik und Physik*, 2016, 67(2), 24.
- [43] Cazzani, A., Stochino, F., Turco, E., On the whole spectrum of timoshenko beams. part ii: further applications, *Zeitschrift für angewandte Mathematik und Physik*, 2016, 67(2), 25.
- [44] Seyranian, A.P., Mailybaev, A.A., *Multiparameter stability theory with mechanical applications*, vol. 13, World Scientific, 2003.
- [45] Silvestre, N., Camotim, D., First-order generalised beam theory for arbitrary orthotropic materials, *Thin-Walled Structures*, 2002, 40(9), 755 – 789.
- [46] Ranzi, G., Luongo, A., A new approach for thin-walled member analysis in the framework of gbt, *Thin-Walled Structures*, 2011, 49(11), 1404 – 1414.
- [47] Taig, G., Ranzi, G., D’Annibale, F., An unconstrained dynamic approach for the generalised beam theory, *Continuum Mechanics and Thermodynamics*, 2015, 27(4-5), 879–904.



ORCID iD

 Manuel Ferretti  <https://orcid.org/0000-0002-7578-6699>

 Francesco D'Annibale  <https://orcid.org/0000-0002-6580-9586>

 Angelo Luongo  <https://orcid.org/0000-0003-1426-7825>


© 2021 by the authors. Licensee SCU, Ahvaz, Iran. This article is an open access article distributed under the terms and conditions of the Creative Commons Attribution-NonCommercial 4.0 International (CC BY-NC 4.0 license) (<http://creativecommons.org/licenses/by-nc/4.0/>)

How to cite this article: Manuel Ferretti, Francesco D'Annibale, Angelo Luongo. Modeling beam-like planar structures by a one-dimensional continuum: an analytical-numerical method, *J. Appl. Comput. Mech.*, 7(SI), 2021, 1020-1033. <https://doi.org/10.22055/JACM.2020.33100.2150>

Appendix A Analytical expressions of the elastic constants in the rigid-floor case

Under the hypothesis of rigid-floor, the following elastic constants have been found in [26, 18, 19, 20, 23] for the equivalent Timoshenko beam:

$$\begin{aligned}
 \frac{C_{11}^{\infty}}{h} &:= \sum_{i=1}^m D_{ci} + \sum_{i=1}^{m-1} (D_{bri}^+ + D_{bri}^-) \sin^2(\beta_i), \\
 \frac{C_{22}^{\infty}}{h} &:= \sum_{i=1}^m S_{ci} + \sum_{i=1}^{m-1} (D_{bri}^+ + D_{bri}^-) \cos^2(\beta_i), \\
 \frac{C_{33}^{\infty}}{h} &:= \sum_{i=1}^m (D_{ci} y_i^2 + B_{ci}) + \sum_{i=1}^{m-1} \left[D_{bri}^+ \left(y_{i+1} \sin(\beta_i) + \frac{h}{2} \cos(\beta_i) \right)^2 + D_{bri}^- \left(y_i \sin(\beta_i) - \frac{h}{2} \cos(\beta_i) \right)^2 \right], \\
 \frac{C_{12}^{\infty}}{h} &:= \sum_{i=1}^{m-1} (D_{bri}^- - D_{bri}^+) \sin(\beta_i) \cos(\beta_i), \\
 \frac{C_{33}^{\infty}}{h} &:= - \sum_{i=1}^m D_{ci} y_i - \sum_{i=1}^{m-1} \sin(\beta_i) \left[D_{bri}^+ \left(y_{i+1} \sin(\beta_i) + \frac{h}{2} \cos(\beta_i) \right) + D_{bri}^- \left(y_i \sin(\beta_i) - \frac{h}{2} \cos(\beta_i) \right) \right], \\
 \frac{C_{23}^{\infty}}{h} &:= \sum_{i=1}^{m-1} \cos(\beta_i) \left[D_{bri}^+ \left(y_{i+1} \sin(\beta_i) + \frac{h}{2} \cos(\beta_i) \right) - D_{bri}^- \left(y_i \sin(\beta_i) - \frac{h}{2} \cos(\beta_i) \right) \right].
 \end{aligned} \tag{23}$$

Here, at each span i , $\beta_i^+ := \arctan(h/b_i) =: \beta_i$, is the an angle of inclination, measured with respect to the horizontal line, of a subset of bracing elements, while the other subset has opposite slope $\beta_i^- = -\beta_i$, and y_i is the coordinate at which the i -th column is located. Moreover, the *global column stiffness coefficients* appear, defined as:

$$D_c = \frac{EA_c}{h}, \quad S_c = \frac{12EJ_c}{(1 + \alpha_c)h^3}, \quad B_c = \frac{EJ_c}{h}, \tag{24}$$

EA_c, GA_c^*, EJ_c being the extensional, shear and flexural local column stiffnesses, and $\alpha_c := \frac{12EJ_c}{GA_c^*h^2}$ is the flexural-to-shear stiffness ratio. Finally, $D_{br} = \frac{EA_{br}}{h_{br}}$ is the global axial stiffness of the bracing elements (superscript + or - denotes the relevant subset of bracing elements), EA_{br}, h_{br} being its local extensional stiffness and length, respectively.

